

Mechanism of thermal decomposition of carbamoyl phosphate and its stabilization by aspartate and ornithine transcarbamoylases

Qin Wang^a, Jiarong Xia^a, Victor Guallar^b, Goran Krilov^a, and Evan R. Kantrowitz^{a,1}

^aDepartment of Chemistry, Merkert Chemistry Center, Boston College, Chestnut Hill, MA 02467; and ^bCatalan Institute for Research and Advanced Studies, Life Science Department, Barcelona Supercomputing Center, Jordi Girona 29, Barcelona 08034, Spain

Communicated by William N. Lipscomb, Harvard University, Cambridge, MA, September 25, 2008 (received for review July 21, 2008)

Carbamoyl phosphate (CP) has a half-life for thermal decomposition of <2 s at 100 °C, yet this critical metabolic intermediate is found even in organisms that grow at 95–100 °C. We show here that the binding of CP to the enzymes aspartate and ornithine transcarbamoylase reduces the rate of thermal decomposition of CP by a factor of >5,000. Both of these transcarbamoylases use an ordered-binding mechanism in which CP binds first, allowing the formation of an enzyme-CP complex. To understand how the enzyme-CP complex is able to stabilize CP we investigated the mechanism of the thermal decomposition of CP in aqueous solution in the absence and presence of enzyme. By quantum mechanics/molecular mechanics calculations we show that the critical step in the thermal decomposition of CP in aqueous solution, in the absence of enzyme, involves the breaking of the C—O bond facilitated by intramolecular proton transfer from the amine to the phosphate. Furthermore, we demonstrate that the binding of CP to the active sites of these enzymes significantly inhibits this process by restricting the accessible conformations of the bound ligand to those disfavoring the reactive geometry. These results not only provide insight into the reaction pathways for the thermal decomposition of free CP in an aqueous solution but also show why these reaction pathways are not accessible when the metabolite is bound to the active sites of these transcarbamoylases.

carbamoyltransferase | quantum mechanics/molecular mechanics | substrate stabilization | thermophile

Carbamoyl phosphate (CP) is a key metabolic intermediate in the biosynthesis of arginine and the pyrimidine nucleotides and for the detoxification of urea. In arginine biosynthesis, the enzyme ornithine (Orn) transcarbamoylase (OTCase) catalyzes the condensation of CP with Orn to form citrulline, an arginine precursor. In pyrimidine nucleotide biosynthesis, the enzyme aspartate transcarbamoylase (ATCase) catalyzes the condensation of CP and L-Asp to form *N*-carbamoyl-L-aspartate (CA).

The quaternary structure of OTCase is a trimer of identical polypeptide chains. In organisms such as *Bacillus subtilis*, ATCase and OTCase have similar trimeric structures. The quaternary structure of ATCase is species-dependent; however, in all species the basic structural unit of the catalytic portion of ATCase is a trimer. The 3 active sites of the catalytic trimer of ATCases and OTCases are located at the subunit interfaces, and residues from the adjacent chain are necessary for catalysis. A sequence alignment of the domain responsible for the binding of CP in ATCases and OTCases suggests a common ancestral gene (1). The structural similarity of the CP domain from the two enzymes has been confirmed by X-ray crystallography (2, 3).

CP is synthesized by the enzyme CP synthetase. This reaction proceeds via the highly unstable intermediates carboxyphosphate and carbamate. *Escherichia coli* CP synthetase has an internal tunnel between active sites that is proposed to channel these intermediates directly from one active site to another without diffusion into solution. The channeling of these inter-

mediates in CP synthetase is a means of protecting them from thermal decomposition (4).

The monoanion and dianion forms of CP are the predominant species between pH 2–4 and 6–8, respectively. Allen and Jones (5) proposed that the monoanion decomposes by P—O bond cleavage, whereas the dianion decomposes by C—O bond cleavage. At physiological pH, CP is thermally unstable with a half-life ($t_{1/2}$) of ≈ 5 min at 37 °C. At neutral pH, the primary decomposition product of CP is cyanate, a promiscuous alkylating agent (5) (see Scheme 1). The thermal instability of CP is a more acute problem for thermophilic organisms that grow at temperatures as high as 95–100 °C, where the $t_{1/2}$ for the thermal decomposition of CP is <2 s (6). Hence, there must be an intracellular mechanism or mechanisms for the protection of CP from thermal decomposition. In the hyperthermophilic organism *Aquifex aeolicus*, channeling of CP between CP synthetase and ATCase has been established (7).

Analysis of the structural data for human OTCase revealed a molecule of CP bound in the active site even though CP had not been added to the crystallization buffer (8). The source of the CP was traced to its use during the purification of the enzyme weeks before. This result suggested that the OTCase was able to protect CP from thermal decomposition.

The enzymatic mechanism of the transcarbamoylation reaction by OTCase and ATCase is ordered, with CP binding before Asp/Orn and CA/citrulline leaving before P_i (9, 10), which allows these enzymes to bind CP in the absence of Asp/Orn. The constants for binding of CP to ATCases and OTCases are similar, ranging from 4 to 10 μ M (11, 12). Here, we use a combination of enzymatic studies and computational modeling to evaluate the hypothesis that the binding of CP to the active site of OTCase and ATCase provides a mode of protecting CP from thermal decomposition. Furthermore, through extensive quantum mechanical and quantum mechanics/molecular mechanics (QM/MM) calculations, we provide insight into the mechanism of thermal decomposition of free CP in aqueous solution and show why these reaction pathways are not accessible when the CP is bound to the active sites of these transcarbamoylases.

Results and Discussion

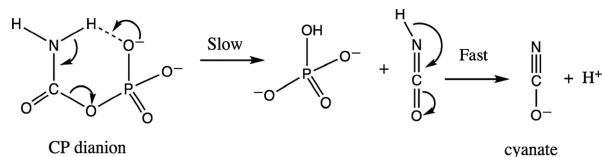
Thermal Stability of Free and Enzyme-Bound CP. To establish a reference, the thermal stability of free CP was first determined under conditions identical to those used in later experiments with the enzymes. Samples of CP in a buffered aqueous solution were incubated for 5 min at temperatures between 5 °C and 95 °C. After quenching the reaction, the amount of CP remain-

Author contributions: V.G., G.K., and E.R.K. designed research; Q.W., J.X., V.G., G.K., and E.R.K. performed research; Q.W., J.X., V.G., G.K., and E.R.K. analyzed data; and V.G., G.K., and E.R.K. wrote the paper.

The authors declare no conflict of interest.

¹To whom correspondence should be addressed. E-mail: evan.kantrowitz@bc.edu.

© 2008 by The National Academy of Sciences of the USA



Scheme 1. Proposed thermal decomposition of CP.

ing was determined. The percentage of CP remaining as a function of temperature is shown in Fig. 1.

To determine whether transcarbamoylases can enhance the thermal stability of CP, samples of CP were incubated in the presence of ATCase at different active site/CP ratios for 5 min at 45 °C. When the active site/CP ratio was ≥ 1 , maximum protection of the CP was observed. However, at lower active site/CP ratios, the amount of protection afforded by the enzyme was reduced in proportion to the number of enzyme active sites.

As shown in Fig. 1, both ATCase and OTCase are able to protect CP from thermal decomposition up to ≈ 65 °C, which is the temperature at which these enzymes begin to denature (see below and Table 1). Whereas approximately half of the CP decomposed after a 5-min incubation at 40 °C in the absence of the enzymes, in the presence of either *E. coli* ATCase or OTCase at an active site/CP ratio of 1.0, virtually no decomposition of CP was observed. Moreover, after an incubation of 5 min at 65 °C 90% of the CP decomposed, whereas only 19%, 50%, and 28% of the initial CP decomposed in the presence of *E. coli* ATCase holoenzyme, *E. coli* ATCase catalytic subunit (c_3), and *E. coli* OTCase, respectively.

The c_3 of the thermophilic ATCase from *Methanococcus jannaschii* was used to extend the data in Fig. 1 to higher temperatures. After an incubation at 90 °C for 5 min 80% of the CP was protected from thermal decomposition by the *M. jannaschii* c_3 . However, no CP could be detected after the same treatment in the absence of the enzyme. To show that the protection afforded to CP was specific to these CP binding enzymes, ATCase and OTCase, the experiments were repeated in the presence of the α -amylases from *B. subtilis*, a mesophile, and *Bacillus licheniformis*, a thermophile. These enzymes are stable thermally up to 65 °C and 90 °C, respectively (see Table 1). However, no CP could be detected after incubation with either of these enzymes.

Finally, to determine how effective the enzymes were in protecting CP from thermal decomposition, a prolonged incubation of CP with the *M. jannaschii* ATCase c_3 was carried out at 90 °C. After 60 min, only 20% of the CP was destroyed. This result demonstrated that binding of CP to ATCase can extend the lifetime of CP by $>5,000$ -fold, and that the binding of CP to the active sites of these

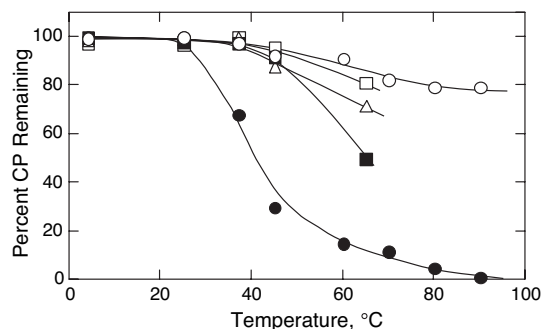


Fig. 1. Percentage of CP remaining after a 5-min incubation in the absence (●) and presence (□) of *E. coli* ATCase holoenzyme, *E. coli* ATCase c_3 (■), *E. coli* OTCase (△), and *M. jannaschii* c_3 (○) as a function of temperature.

Table 1. Thermal stability of the enzymes

Enzyme	T_m , °C	
	No CP	With CP
<i>E. coli</i> ATCase holoenzyme	65	67
<i>E. coli</i> ATCase c_3	62	65
<i>E. coli</i> OTCase	57	57
<i>M. jannaschii</i> ATCase c_3	>90	>90
<i>B. subtilis</i> α -amylase	60	60
<i>B. licheniformis</i> α -amylase	>90	>90

See *Methods* for the experimental procedure used.

transcarbamoylases constitutes a unique mechanism for the stabilization of this key metabolic intermediate.

Thermal Stability of the Enzymes. The thermal stability of *E. coli* ATCase holoenzyme, *E. coli* ATCase c_3 , *M. jannaschii* c_3 , and *B. subtilis* and *B. licheniformis* α -amylase were determined by circular dichroism in both the absence and the presence of CP, and the results are summarized in Table 1. The melting temperature (T_m) for *E. coli* ATCase holoenzyme in the presence of CP was found to be 67 °C. At this temperature, the enzyme was also observed to lose its ability to protect CP. However, the T_m for *E. coli* OTCase was determined to be 57 °C, which is reflected in the reduced ability of *E. coli* OTCase to protect CP as compared with the *E. coli* ATCase holoenzyme. Hence, there appears to be a direct relationship between the thermal stability of the enzymes (*M. jannaschii* c_3 $>$ *E. coli* ATCase holoenzyme $>$ *E. coli* ATCase c_3) and their ability to protect CP from thermal decomposition.

The Mechanism of the Thermal Decomposition of CP. To rationalize the above experimental findings, it is necessary to determine the molecular mechanism by which these enzymes protect CP from thermal decomposition on the atomic level. To accomplish this, it was essential to first obtain a detailed understanding of the thermal decomposition pathways for free CP in solution, and subsequently, how these pathways are modified in the protein environment. A computational approach is particularly suitable for this task, because it provides atomic-level detail to complement the experimental measurements.

The decomposition of the CP dianion has been proposed to proceed by 2-step unimolecular elimination of cyanate via an intramolecular proton transfer to yield the phosphate dianion (5) (see Scheme 1). The proton transfer, a central driving force for the slow, rate-determining step, is believed to be facilitated by the formation of a 6-membered ring structure generated by the establishment of a hydrogen bond between the amino group and a phosphate oxygen. In this conformation, all 6 atoms of the ring are coplanar, and the P—O—C—N dihedral angle is $\approx 0^\circ$. Starting with this initial configuration, the reactive geometry was optimized by density functional theory (DFT) calculations by keeping the P—O—C—N constrained at 0° , while the remaining CP degrees of freedom were allowed to relax. This structure was used as a starting point for a series of DFT calculations* to probe the mechanism of thermal decomposition of CP. The slow step outlined in Scheme 1 involves both the transfer of the proton from the amine nitrogen to the phosphate oxygen and the cleavage of the C—O bond. Because the sequence of these events and the underlying energetics are unknown, we computed the potential energy profile for the CP decomposition as a

*To validate the accuracy of the DFT approach, several of the reported values have been computed by using the MP2 level of theory. In all cases, close agreement with DFT results within 0.5 kcal/mol was observed.

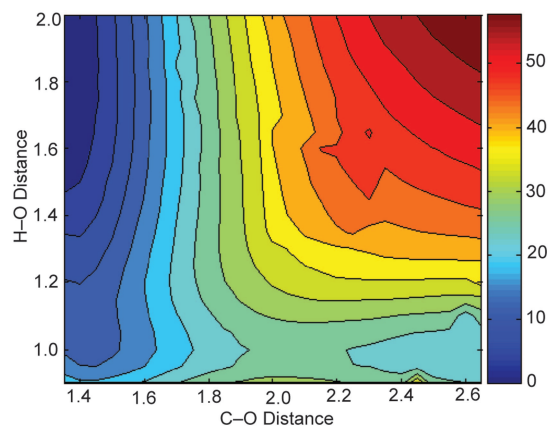


Fig. 2. Contour plot of the 2D potential energy surface describing the thermal decomposition of CP as a function of C—O distance and H—O distance (Å). Color map indicates the energy in kcal/mol relative to the reactant geometry.

function of 2 reaction coordinates: the C—O distance and the distance of the amine proton to the accepting oxygen. The resulting 2D potential energy surface for the thermal decomposition of CP is shown in Fig. 2. The basin in the upper left portion of the surface in Fig. 2 corresponds to the optimized 6-membered ring state, with optimized C—O and H—O distances of 1.35 and 1.95 Å, respectively. A second, higher-lying basin, corresponding to the products of the slow reaction in Scheme 1, with the C—O bond cleaved and the proton fully transferred to the leaving phosphate, is located in the lower right portion of Fig. 2, centered at a C—O distance of ≈ 2.6 Å and the newly formed H—O bond length of ≈ 0.95 Å. The 2 basins are connected by a broad saddle transition region. To explore this surface in more detail, in Fig. 3A the energy profiles for the proton transfer as a function of H—O distance are shown, for several values of the C—O distances. At the equilibrium C—O bond length, the proton transfer is clearly not favored, with the energy profile exhibiting a steady increase in energy as the H—O distance is reduced, leading to a destabilization of ≈ 17 kcal/mol. The transfer remains unfavorable, although progressively less so with increasing C—O distance, until the latter reaches ≈ 1.65 Å, at which point the proton transfer is approximately energetically neutral. For larger C—O distances, the proton transfer becomes increasingly favorable, with an energy gain approaching ≈ 37 kcal/mol for C—O distance of 2.55 Å, by which stage the C—O bond is clearly broken. However, examination of the energy profiles along the C—O reaction coordinate for fixed values of H—O distance (Fig. 3B) shows that the proton transfer is necessary for the formation of stable thermal decomposition products (first observed at a H—O distance of ≈ 1.1 Å) and also contributes to the reduction of the activation barrier for C—O bond cleavage by ≈ 30 kcal/mol.

Overall, these results indicate that the key step in the thermal decomposition of CP proceeds via an intramolecular proton transfer activated by the thermal fluctuations of the C—O bond, which drives the cleavage of the latter through a saddle-point transition state located approximately at the C—O and H—O distance of ≈ 1.8 and ≈ 1.2 Å, respectively. The slow step of the decomposition reaction is endothermic, with $\Delta E = 21$ kcal/mol and an activation barrier of ≈ 25 kcal/mol. Note that for this thermal decomposition mechanism to be energetically feasible both the activation of the C—O bond cleavage through thermal fluctuations and the proton transfer are required.

Stabilization of CP by the Enzyme Active Site. Based on the above results, the Allen–Jones mechanism (5) for thermal decompo-

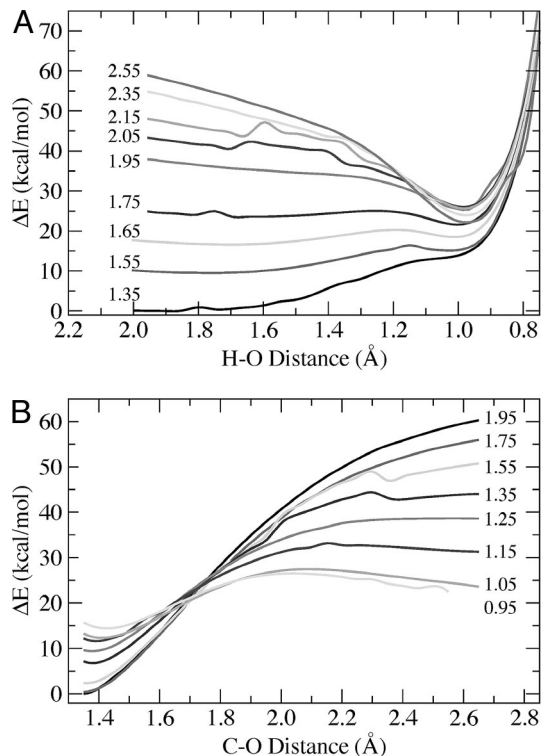


Fig. 3. Potential energy surfaces for thermal decomposition of CP in water along 2 relevant reaction coordinates. (A) Energy profiles for the proton transfer as a function of H—O distance between the amine proton and the phosphate oxygen acceptor, measured relative to the energy of the optimized reactive configuration. Different curves correspond to specific values of the C—O distance shown beside each curve. (B) Energy profiles for the C—O bond cleavage as a function of the C—O distance, measured relative to the energy of the optimized reactive configuration. Different curves correspond to specific values of the H—O distance of the transferring proton, shown beside each curve.

sition of CP requires 2 conditions: (i) the adoption of the 6-membered planar ring reactive geometry, and (ii) subsequent cleavage of the C—O bond and the accompanying proton transfer. Hence, the preclusion of either of these for CP bound in the active site of the enzyme would constitute an adequate mode of protection vs. thermal decomposition. To assess the relative stability of the 6-membered ring reactive geometry for the free solution form of CP, a series of DFT calculations were performed to obtain the torsional energy profile for the P—O—C—N dihedral rotation (Fig. 4). The minimum energy conformation was found at a P—O—C—N dihedral angle of $\approx 0^\circ$, confirming that the reactive geometry is the preferred conformation for free CP in aqueous solution. A second stable conformation, corresponding to the extended form of CP and lying 3 kcal/mol higher in energy, was observed at a P—O—C—N dihedral angle of $\approx 180^\circ$, separated from the minimum energy conformation by a ≈ 6 kcal/mol torsional rotational barrier. Hence, free CP in solution appears to be predisposed conformationally toward decomposition via the Allen–Jones pathway (5).

However, the crystal structures of the complexes of CP with *E. coli* ATCase (13) and human OTCase (8) show that CP prefers the extended structure when bound in the active sites of these enzymes, with a P—O—C—N dihedral angle of 179.9° and 173.3° , respectively (Fig. 5). Multiple bonding interactions favor this conformation. To determine whether the reactive geometry is accessible in the active site of the protein, a series of QM/MM optimizations were performed to compute the torsional energy

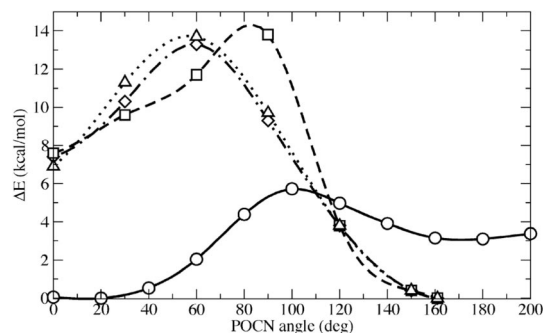


Fig. 4. The energy profile along the P—O—C—N dihedral angle for free CP in water (○) and for CP bound to the active site of *E. coli* ATCase. The energies are measured relative to the minimum energy conformation. Three separate sweeps along the reaction coordinate were performed for the protein-bound CP: starting from extended structure ($\approx 180^\circ$) to the reactive geometry ($\approx 0^\circ$) (◊); back to the extended structure (◻), and once again to the ring structure (Δ).

profile along the P—O—C—N dihedral angle. In each case, CP was treated quantum mechanically, whereas the protein and solvent were treated classically. Starting with the crystal structure coordinates, a full QM/MM optimization yielded an energy-minimized structure with the P—O—C—N dihedral angle close to 180°. To enhance the QM/MM sampling, 3 scans of the reaction coordinate were calculated along the said dihedral angle, from the initial minimized structure (P—O—C—N angle 180°) to 0°, then back to 180°, and then back again to 0°. The energy profiles, shown in Fig. 4, clearly indicate that the enzyme hinders the reactive conformation. The energy barrier for interconversion was found to be ≈ 13.5 kcal/mol, significantly larger than the one observed for free CP in solution. Furthermore, the energy difference between the 2 stable conformers of ≈ 7 kcal/mol indicates a strong preference for the extended conformers. These results suggest that the reactive ring geometry is inaccessible at moderately high temperatures considered in this study. The variation in conformational preferences for CP between the protein and the aqueous environment might be explained by the hydrogen-bond network in the protein active site. Fig. 6 shows the hydrogen-bonding interactions for both the extended and the ring-like conformers, after the QM/MM optimization. The principal differences are observed at the carbamoyl end of the ligand, where transition to the ring-like conformer results in a loss of both hydrogen bonds with the

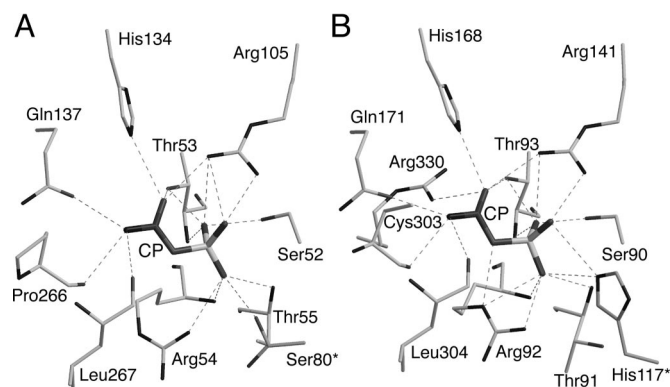


Fig. 5. X-ray structure of CP bound in the active site of ATCase (PDB ID code 1ZA2) (13) (A) and CP bound in the active site of OTCase (PDB code 1EP9) (8) (B). Sixteen and 19 hydrogen bonds constrain the conformation of CP in the active sites of ATCase and OTCase, respectively. The asterisks after Ser-80 (ATCase) and His-117 (OTCase) indicate that these residues are donated into the active site from the adjacent chain.

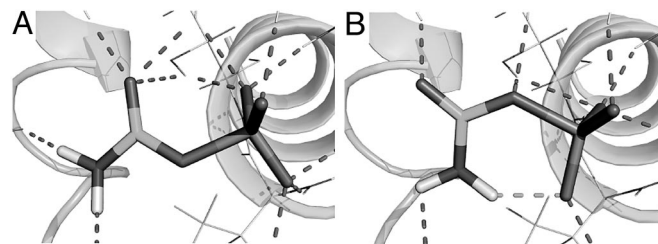


Fig. 6. Hydrogen bond network of CP in the active site of ATCase, after QM/MM optimization for the 180° (A) and the 0° (B) dihedral conformers. Hydrogen bonds are shown in a dotted line. The CP ligand is shown in the center with a stick representation.

amine and one with the carbonyl oxygen. To further explore possible local conformational changes that might modify this pattern, 1.5 ns of molecular dynamics at 300 K was performed, keeping the dihedral constrained at 0° by using a potential similar to the one used in QM/MM calculations. No significant change in the hydrogen-bond pattern was observed. Indeed, the structure shown in Fig. 6B is derived from the final snapshot of this MD simulation, after a QM/MM reoptimization.

We next considered the potential for the cleavage of the C—O bond of CP in the protein active site. Starting with the optimized ring conformation shown in Fig. 6A, constrained QM/MM calculations were performed at various C—O distances. The resulting energy profile measured relative to the initial structure is shown in Fig. 7. The proton transfer was observed to be spontaneous at C—O distances >1.8 Å, corresponding to the transition state. For C—O distances >2.4 Å, the C—O bond was found to be fully cleaved, and the proton transfer was complete after the QM/MM optimization. These findings are qualitatively similar to the reaction profiles for the decomposition of free CP observed in a continuum solvent, although the activation energy and endothermicity are slightly increased in the protein. In summary, binding of CP to the protein active site appears to confer resistance to thermal decomposition primarily by restricting the accessible conformations of the ligand to the extended form, thereby precluding the formation of the hydrogen-bonded 6-membered ring precursor required for the proton transfer-coupled C—O bond cleavage reaction.

Conclusions

The binding of an inhibitor or product into the active site of enzymes often improves the stability of the enzyme in vitro. This improved stability is frequently the result of enhanced rigidity of the protein caused by formation of the complex. Enzymes such as triose-phosphate isomerase (14) and bacterial benzoylformate

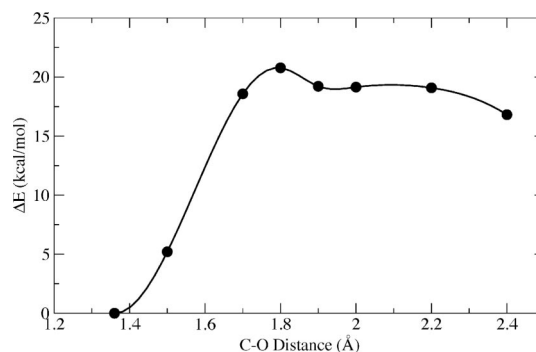


Fig. 7. The energy profile for the cleavage of the C—O bond of CP bound to the active site of *E. coli* ATCase, as a function of the C—O distance, measured relative to the energy of the optimized reactive configuration.

decarboxylase (15) are also known to stabilize key reaction intermediates. In this study, we examined how the formation of a complex between an enzyme and a small molecule can protect the small molecule from decomposition. If the binding of the small molecule to the protein alters the environment of the small molecule (e.g., excludes water) hydrolysis of the small molecule may be slowed. It is well known that CP is a critical metabolite for both arginine and pyrimidine biosynthesis, yet the short half-life of this molecule ($t_{1/2} < 2$ s at 100 °C) seems to necessitate some special mode of stabilization, especially in thermophilic organisms. Passing of metabolic intermediates between 2 enzymes that form permanent or transient complexes is one method of extending the lifetime of metabolic intermediates (6, 7, 16, 17). However, the decomposition mechanism of the dianion of CP, which would exist under physiological conditions, proceeds through a unimolecular reaction involving an intramolecular C—O bond breaking, thus a mechanism of protection must be more complex than a simple exclusion of water. To rationalize the experimental observation that the binding of CP to transcarbamoylases can reduce the rate of thermal decomposition by a factor of 5,000 or more, we used a combination of quantum mechanical and classical molecular mechanics calculations to characterize the mechanism of decomposition of the CP dianion both in free solution form and bound to ATCase active site.

The quantum mechanical potential energy surface computed along the putative thermal decomposition pathways of CP confirms that the decomposition of CP involves an intramolecular proton transfer facilitated by the formation of a hydrogen-bonded 6-membered ring structure, as originally proposed by Allen and Jones (5). Our calculations show that the preferred conformation of CP in water corresponds to a P—O—C—N dihedral angle of 0°, a geometry that allows formation of the 6-membered hydrogen-bonded ring structure necessary to the intramolecular transfer of an amide proton to a phosphate oxygen. Allen and Jones also proposed that, in addition to proton transfer, the decomposition of the CP dianion requires the cleavage of the C—O bond to eliminate cyanate, leading to the formation of the phosphate dianion (5). This mechanism is consistent with the observed absence of ^{18}O incorporation into phosphate in isotope studies and the absence of salt effects. However, it still remains uncertain whether the driving force for the decomposition of CP is the proton transfer itself, or if it is the breaking of the C—O bond. Our results indicate that whereas the activation of the C—O bond through thermal fluctuations is the critical and necessary step in the decomposition mechanism of CP in water, much of the driving force for the cleavage of the bond is derived from the proton transfer, which becomes energetically feasible once the bond is partially broken. As the saddle-point nature of the transition state suggests, the breaking of the C—O bond and the formation of the H—O bond are likely coupled, because a phosphate monoanion intermediate would be unstable at this pH.

However, our QM/MM calculations clearly demonstrate that the enzyme stabilizes CP from thermal decomposition by inhibiting the Allen–Jones pathway (5). The 16 hydrogen-bonding interactions with the protein restrict CP to conformations that are strongly unfavorable for a concerted C—O bond breaking and proton transfer, with a P—O—C—N dihedral close to 180°. This dihedral angle is far removed from the 0° dihedral angle that would permit formation of the 6-membered hydrogen-bonded ring structure involved in the thermal decomposition pathway of CP in water. This mechanism of protection of CP from thermal decomposition likely extends to other transcarbamoylases. Not only are the structures of the CP binding sites in ATCase and OTCase virtually identical (compare Fig. 5 *A* and *B*), but the conformations of CP bound in the active sites of the 2 enzymes are also very similar. Furthermore, in the OTCase–CP structure

(8) there are even more hydrogen-bonding interactions (19 to be exact) constraining the CP in its extended conformation compared with the ATCase–CP complex (which has 16), hence a higher barrier toward dihedral rotation required to achieve the reactive geometry would be expected.

Although there is no high-resolution structural data for *M. jannaschii* ATCase, the residues determined to be critical for binding CP in *E. coli* ATCase are all conserved in the *M. jannaschii* ATCase (18). Homology modeling of the structure of *M. jannaschii* ATCase also indicates that the active site has a 3D structure very similar to that of *E. coli* ATCase (18). These data suggest that the active site in *M. jannaschii* ATCase can also constrain the geometry of CP in a conformation that is unfavorable to thermal decomposition and likely also stabilizes the C—O bond.

Although the basic structure of the transcarbamoylases provides stability to CP bound in the active site, this mechanism for the thermal protection of CP may be only one of many that are used in thermophilic organisms. In the case of *M. jannaschii* ATCase, further studies are required to determine whether channeling of CP via complex formation between CP synthetase and ATCase and OTCase provide alternative modes of protection of CP from thermal decomposition. Other modes of protection of CP can now be studied based on the effects of the local physiological medium. Also, the medium used in crystallographic studies may partially stabilize CP even in the absence of the enzyme as observed in NMR experiments (figure 1 in ref. 19).

Methods

Enzyme Preparation. *E. coli* ATCase holoenzyme and c_3 were overexpressed by using *E. coli* strain EK1104 (20) containing plasmids pEK152 and pEK17, respectively. The isolation and purification were as described (20). *E. coli* OTCase and the c_3 of *M. jannaschii* ATCase were overexpressed and purified as described (1, 18).

Thermal Decomposition Measurements in the Absence and Presence of Enzyme.

To determine the ability of ATCase and OTCase to protect CP from thermal decomposition, CP was incubated in the absence and presence of ATCase and OTCase for 5 min at temperatures ranging from 5 °C to 65 °C in 100 mM Tris–acetate buffer (pH 8.3). The reactions were quenched on ice before the determination of the amount of CP remaining. The latter was measured by adding a large excess of aspartate and ATCase (if required) followed by incubation for 30 min at 25 °C. The amount of CA formed was determined colorimetrically (21).

Protein Stability Measurements. The thermal stability of the enzymes used was determined through T_m measurements by circular dichroism using an AVIV circular dichroism spectrophotometer. The enzymes (concentration 0.04 mg/ml) were heated at a rate of 2 °C/min in a 0.1 M Tris–acetate buffer (pH 8.3), in the absence and in presence of 1 mole of CP per mole of active sites.

Computational Methods. Quantum mechanical calculations at the DFT level were used to generate the 2D potential energy surface for the cleavage of the C—O bond for free CP in the aqueous solution, as a function of 2 reaction coordinates: the C—O distance and the distance between the amine H and nearest phosphate O. All calculations were performed by using the B3LYP functional (22) and the 6-311++g** basis set as implemented in Gaussian03 (23). The solvent was treated at the reaction field level by using the Polarizable Continuum model (24, 25) with the UA0 united atom topology as implemented in Gaussian03. The C—O bond lengths were sampled from 1.35 to 2.65 Å in 0.05-Å increments, and the H—O distances were sampled from 2.0 Å decreasing to 0.85 Å in 0.05-Å increments. For each point, the values of the 2 reaction coordinates were constrained, whereas all other degrees of freedom were fully optimized. In a separate calculation, the potential energy profile along the P—O—C—N dihedral angle reaction coordinate was obtained by using the same method by constraining the former at 20° intervals from 0° to 180°.

QM/MM approaches join the quantum and classical treatments of different portions of a complex condensed phase system, thereby permitting proper description of the potential energy surfaces relevant to enzymatic chemistry and to accurate treatment the polarization of the quantum region. The active site is treated with a robust ab initio quantum mechanical methodology. The

remainder of the protein can be modeled at the molecular mechanics level, providing the appropriate interactions with the core reactive region. All QM/MM calculations were performed with Qsite (Schrödinger) by using the DFT B3LYP level of theory and the 6–311G* basis set. The classical mechanical region is described by the all-atom OPLS2001 force field (26, 27). A detailed description of the QM/MM methods and protocols can be found in previous studies (28). The QM/MM model was constructed from the X-ray structure of the enzyme-CP complex [Protein Data Bank (PDB) ID code 1ZA2 (13)]. A close inspection of the crystal structure indicated that histidines 170, 106, 265, 134, and 8 should be protonated in their ϵ position. The system was soaked in a box of simple point charge (SPC) water molecules (29) and equilibrated following the protocol described (30). For the final QM/MM model only those atoms within 25 Å from the CP molecule were retained. Default values for convergence criteria were used, and all nonbonded interactions were truncated at 25 Å. In each QM/MM calculation, the aforementioned dihedral angle was

constrained, whereas all atoms within 22 Å of the ligand were allowed to optimize.

The molecular dynamics simulations of the ATCase-CP complex were performed by using IMPACT (Schrödinger). The potential parameters for the protein and CP were assigned from the all-atom OPLS 2001 force field, except for the CP partial charges, which were derived from QM/MM calculations. Nose-Hoover thermostats were used to maintain the temperature at 298 K, and only atoms within 22 Å of CP were permitted to move. All nonbonded interactions were truncated at 25 Å. Following a standard equilibration protocol, a 1.5-ns trajectory was evolved at a constant number of particles, volume, and temperature with a time step of 1 fs.

ACKNOWLEDGMENTS. This work was supported by National Institutes of Health Grant GM26237 (to E.R.K.), a startup grant from Boston College (to G.K.), and the Barcelona Supercomputing Center (V.G.).

- Labedan B, et al. (1999) The evolutionary history of carbamoyltransferases: A complex set of paralogous genes was already present in the last universal common ancestor. *J Mol Evol* 49:461–473.
- Kim KH, Pan Z, Honzatko RB, Ke H-M, Lipscomb WN (1987) Structural asymmetry in the CTP-liganded form of aspartate carbamoyltransferase from *Escherichia coli*. *J Mol Biol* 196:853–875.
- Jin L, Seaton BA, Head JF (1997) The crystal structure of anabolic *Escherichia coli* ornithine transcarbamylase at 2.8-Å resolution. *Nat Struct Biol* 4:622–625.
- Thoden JB, Holden HM, Wesenberg G, Rauschel FM, Rayment I (1997) Structure of carbamoyl phosphate synthetase: A journey of 96 Å from substrate to product. *Biochemistry* 36:6305–6316.
- Allen CM, Jr, Jones ME (1964) Decomposition of carbamylphosphate in aqueous solution. *Biochemistry* 3:1238–1247.
- Legrain C, Demarez M, Glansdorff N, Piérard A (1995) Ammonia-dependent synthesis and metabolic channelling of carbamoyl phosphate in the hyperthermophilic archaeon *Pyrococcus furiosus*. *Microbiology* 141:1093–1099.
- Purcarec C, et al. (2003) *Aquifex aeolicus* aspartate transcarbamoylase, an enzyme specialized for the efficient utilization of unstable carbamoyl phosphate at elevated temperature. *J Biol Chem* 278:52924–52934.
- Shi D, et al. (2001) Human ornithine transcarbamylase: Crystallographic insights into substrate recognition and conformational changes. *Biochem J* 354:501–509.
- Hsuanyu Y, Wedler FC (1987) Kinetic mechanism of native *Escherichia coli* aspartate transcarbamylase. *Arch Biochem Biophys* 259:316–330.
- Parmentier LE, Kristensen JS (1998) Studies on the urea cycle enzyme ornithine transcarbamylase using heavy atom isotope effects. *Biochim Biophys Acta* 1382:333–338.
- Ridge JA, Roberts F, Schaffer MH, Stark GR (1976) Aspartate transcarbamylase of *Escherichia coli*. Heterogeneity of binding sites for carbamyl phosphate and fluorinated analogs of carbamyl phosphate. *J Biol Chem* 251:5966–5975.
- Zambidis I, Kuo LC (1990) Substrate specificity and protonation state of *Escherichia coli* ornithine transcarbamoylase as determined by pH studies. Binding of carbamoyl phosphate. *J Biol Chem* 265:2620–2623.
- Wang J, Stieglitz KA, Cardia JP, Kantrowitz ER (2005) Structural basis for ordered substrate binding and cooperativity in aspartate transcarbamoylase. *Proc Natl Acad Sci USA* 102:8881–8886.
- Richard JP (1991) Kinetic parameters for the elimination reaction catalyzed by triose-phosphate isomerase and an estimation of the reaction's physiological significance. *Biochemistry* 30:4581–4585.
- Hu Q, Kluger R (2002) Reactivity of intermediates in benzoylformate decarboxylase: Avoiding the path to destruction. *J Am Chem Soc* 124:14858–14859.
- Massant J, Glansdorff N (2004) Metabolic channeling of carbamoyl phosphate in the hyperthermophilic archaeon *Pyrococcus furiosus*: Dynamic enzyme-enzyme interactions involved in the formation of the channeling complex. *Biochem Soc Trans* 32:306–309.
- Purcarec C, Evans DR, Hervé G (1999) Channeling of carbamoyl phosphate to the pyrimidine and arginine biosynthetic pathways in the deep sea hyperthermophilic archaeon *Pyrococcus abyssi*. *J Biol Chem* 274:6122–6129.
- Hack ES, et al. (2000) Characterization of the aspartate transcarbamoylase from *Methanococcus jannaschii*. *J Biol Chem* 275:15820–15827.
- Huang J, Lipscomb WN (2006) T-state active site of aspartate transcarbamylase: Crystal structure of the carbamyl phosphate and L-alanine ligated enzyme. *Biochemistry* 45:346–352.
- Nowlan SF, Kantrowitz ER (1985) Superproduction and rapid purification of *E. coli* aspartate transcarbamoylase and its catalytic subunit under extreme derepression of the pyrimidine pathway. *J Biol Chem* 260:14712–14716.
- Pastra-Landis SC, Foote J, Kantrowitz ER (1981) An improved colorimetric assay for aspartate and ornithine transcarbamylases. *Anal Biochem* 118:358–363.
- Stephens PJ, Devlin FJ, Chabalowski CF, Frisch MJ (1994) Ab initio calculation of vibrational absorption and circular-dichroism spectra using density-functional force fields. *J Phys Chem* 98:11623–11627.
- Frisch MJ, et al. (2004) Gaussian 03 (Gaussian, Wallingford CT), revision c.02.
- Cossi M, Scalmani G, Rega N, Barone V (2002) New developments in the polarizable continuum model for quantum mechanical and classical calculations on molecules in solution. *J Chem Phys* 117:43–54.
- Miertus S, Scrocco E, Tomasi J (1981) Electrostatic interaction of a solute with a continuum: A direct utilization of ab initio molecular potentials for the prevision of solvent effects. *Chem Phys* 55:117–129.
- Jorgensen WL, Maxwell DS, TiradoRives J (1996) Development and testing of the OPLS all-atom force field on conformational energetics and properties of organic liquids. *J Am Chem Soc* 118:11225–11236.
- Kaminski GA, Friesner RA, Tirado-Rives J, Jorgensen WL (2001) Evaluation and reparametrization of the OPLS-AA force field for proteins via comparison with accurate quantum chemical calculations on peptides. *J Phys Chem B* 105:6474–6487.
- Friesner RA, Guallar V (2005) Ab initio quantum chemical and mixed quantum mechanics/molecular mechanics (QM/MM) methods for studying enzymatic catalysis. *Annu Rev Phys Chem* 56:389–427.
- Hermans J, Berendsen HJC, Vangunsteren WF, Postma JPM (1984) A consistent empirical potential for water-protein interactions. *Biopolymers* 23:1513–1518.
- Guallar V, Borrelli KW (2005) A binding mechanism in protein-nucleotide interactions: Implication for U1A RNA binding. *Proc Natl Acad Sci USA* 102:3954–3959.